Molecular Crystals and Liquid Crystals
Publication details, including instructions for authors and subscription information:
http://www.tandfonline.com/loi/gmcl20

Synthesis of TiO_2 Nanotube by Hydrothermal Method and Application for Dye-Sensitized Solar Cell

Chang Hyo Lee [a], Kyung Hwan Kim [a], Kyung Uk Jang [a], Sang Jun Park [b] & Hyung Wook Choi [a]

[a] Department of Electrical Engineering, Kyungwon University San 65 Bokjeong-dong, Sujeong-gu, Seongnam, Gyeonggi-do, Korea

[b] Division of Energy and Biological Engineering, Kyungwon University San 65 Bokjeong-dong, Sujeong-gu, Seongnam, Gyeonggi-do, Korea

Version of record first published: 16 May 2011

To cite this article: Chang Hyo Lee, Kyung Hwan Kim, Kyung Uk Jang, Sang Jun Park & Hyung Wook Choi (2011): Synthesis of TiO_2 Nanotube by Hydrothermal Method and Application for Dye-Sensitized Solar Cell, Molecular Crystals and Liquid Crystals, 539:1, 125/[465]-132/[472]

To link to this article: http://dx.doi.org/10.1080/15421406.2011.566078

Mol. Cryst. Liq. Cryst., Vol. 539: pp. 125/[465]–132/[472], 2011

ISSN: 1542-1406 print/1563-5287 online
DOI: 10.1080/15421406.2011.566078

Taylor & Francis
Taylor & Francis Group

Synthesis of TiO_2 Nanotube by Hydrothermal Method and Application for Dye-Sensitized Solar Cell

CHANG HYO LEE,[1] KYUNG HWAN KIM,[1] KYUNG UK JANG,[1] SANG JUN PARK,[2] AND HYUNG WOOK CHOI[1]

[1]Department of Electrical Engineering, Kyungwon University San 65 Bokjeong-dong, Sujeong-gu, Seongnam, Gyeonggi-do, Korea
[2]Division of Energy and Biological Engineering, Kyungwon University San 65 Bokjeong-dong, Sujeong-gu, Seongnam, Gyeonggi-do, Korea

The TiO_2 nanotube was synthesized by a hydrothermal method dependent on temperature. TiO_2 nanotube was coated on FTO glass by screen printing The TiO_2 nanotube was increasing as autoclaving temperature. The dye-sensitized solar cells were fabricated using ruthenium (II)(N719) dye and electrolyte (I_3/I_3^-). The crystalline structure and morphology were characterized by X-ray diffraction (XRD), and scanning electron microscopy (SEM). The absorption spectra were measured by UV-vis spectrometer. The conversion efficiency was measured by solar simulator. The size and structure of TiO_2 nanotube were adjusted by hydrothermal temperatures. It was found that the conversion efficiency of DSSC was highly affected by the properties of TNT. The diameter of the TiO_2 particles depends on the different hydrothermal temperatures.

Keywords Dye-sensitized solar cell; hydrothermal method; TiO_2 nanotube

Introduction

Dye-sensitized solar cells (DSSCs) have been intensively studied following the discovery of DSSCs in 1991. DSSCs have been extensively researched over the past decades due to their high-energy-conversion efficiency and especially low production cost as cheaper alternatives to silicon solar cells [1,2]. Significant progress has been made recently to enhance the efficiency, including novel sensitized dyes, electrolytes, and photoanode (nanocrystalline metal oxide films) [3]. The photoanodes are commonly a three-dimensional network of interconnected TiO_2 nanoparticles, the band gap of which matches the sensitized dyes. TiO_2 photoanodes are also characterized by low cost and environmental design. The morphology of TiO_2 can be widely tuned to achieve the best efficiency. Grätzel et al. introduced mesoporous TiO_2 particular

Address correspondence to Hyung Wook Choi, Kyungwon University, Bokjeong-dong, Sujeong-gu, Seongnam 461-701, Korea (ROK). Tel.: (+82)31-750-5562; Fax: (+82)31-750-5491; E-mail: chw@kyungwon.ac.kr

films as photoanodes to enhance the effective surface area so as to absorb more dye molecules and thus achieve more light absorption and greater efficiency. However, as the mesoporous TiO_2 particles are randomly connected, this will unavoidably lead to the recombination of electron–hole pairs, decreasing efficiency. Subsequently, researchers started to explore the application of ordinal TiO_2 in the DSSCs; this includes TiO_2 nanowires, nanorods and nanotubes (NTs) [4,5]. TiO_2 nanoparticle films have been used as the photoelectrode in DSSC due to its high specific surface area that allows the adsorption of a large number of dye molecules. These nanoparticles have been prepared by several synthetic routes in a variety of particle sizes, pore size distributions and crystallinities. These factors affect electron transport and consequently, the charge recombination kinetics and the dark current of these cells. In addition, the electron diffusion coefficient determined by laser flash-induced transient photocurrent measurement [6,7] and intensity-modulated photocurrent spectroscopy for TiO_2 nanoparticles [8,9] was more than two orders of magnitude lower than for bulk anatase. The decrease in the electron diffusion coefficient can be a consequence of the presence of electron traps that occur in the grain boundaries at the contacts between the nanoparticles. Thus, the use of oxide semiconductors in the form of nanorods, nanowires and nanotubes may be an interesting approach to improve electron transport through the film. Due to the one-dimensional nature of these nanostructures, their morphology facilitates the electron transfer up to the collecting electrode, decreasing the ohmic loss through the TiO_2 nanorod. In addition, a high level of dye adsorption on the TiO_2 nanorod is expected due to the high surface area presented in these nanostructures [10,11]. The introduction of TiO_2 nanotubes, with a much more open structure, allows the polymer electrolyte to penetrate easily inside the film, increasing the interfacial contact between the nanotubes/dye and the electrolyte. Conversely, the high surface area of TiO_2 nanotubes also allows more sensitize dyes to be chemically attached to the semiconductor surface. In this work, TiO_2 nanotubes were prepared hydrothermically with different temperatures. DSSC was fabricated using prepared TNT.

Experiment

The TiO_2 power was prepared by the sol gel method. The synthesis procedure for the nano TiO_2 is as follows: titanium (IV) tetra ispropoxide [TTIP(Aldrich Chemical)], nitric acid, ethanol, and distilled water were combined. The prepared sol was dried to yield TiO_2 powder. The TiO_2 powder was calcinated in air at 450°C for 1 h using a programmable furnace to obtain the desired stoichiometry and crystallinity of the TiO_2. 10 g of the TiO_2 powders prepared by sol gel method were mixed with 500 ml of NaOH aqueous solution with the concentration of 10 mol, followed by hydrothermal treatment at 120°C, 150°C and 200°C in a Teflon-lined autoclave for 12 h. The treated powders were washed thoroughly with distilled water and 0.1 M HCl several times and subsequently filtered and dried at 80°C for 1 day. The products were calcined at 450°C in air for 1 h.

The prepared paste was then coated onto FTO conductive glass using the screen printing. The TNT films were calcinated in air at 450°C for 1 h using a programmable furnace to obtain the desired stoichiometry and crystallinity of the TiO_2. The nanoporous TiO_2 films were immersed into the dye (N719) complex for 24 h at room temperature. A counter electrode was prepared by dropping an H_2PtCl_6 solution onto FTO glass and heating at 450°C for 30 min. The dye-adsorbed TiO_2 electrode

and the PT counter electrode were assembled into a sandwich type cell and sealed with a hot-melt sealant 50 μm thick. An electrolyte solution was introduced through a drilled hole in the counter electrode. The hole was then sealed using a cover glass.

The phase identification of the particles obtained at various hydrothermal temperatures was performed by X-ray diffraction (XRD) using a Rigaku D/MAX-2200 diffractometer with CuKα radiation. The morphology and the thickness of the prepared TNT layers were investigated using field-emission scanning electron microscopy (FE-SEM, model S-4700, HITACHI). The absorption spectra TNT films were measured by UV-vis spectrometer (UV-vis 8453, Agilent). The conversion efficiency of the fabricated DSSC was measured with an I-V Solar simulator (Solar simulator, Oriel).

Results and Discussions

Figure 1 shows the XRD pattern of the sol gel TiO_2 powders at 450°C are a mixture of the anatase and rutile phases. Figure 2 shows the XRD patterns of the TNT films prepared at various hydrothermal temperatures. The TNT-A (120°C) are a mixture of anatase and rutile phases. The XRD pattern of TNT-B (150°C) shows a prominent anatase peak 25.4°C(101), 48°C(200). However, The XRD pattern of TNT-C (200°C) shows a prominent rutile peak 27.4°C (110), 54.2°C (211). At TNT-C, the anatase peaks nearly disappear, while the intensities of the rutile peaks considerably increase, indicating that the transformation from anatase to rutile is complete. The TiO_2 films were observed to transform into the rutile phase, which has a more stabile structure, as the temperature increases. We find that the crystallized direction intensity changes under different hydrothermal temperatures.

The FE-SEM images of TiO_2 layers prepared at various working pressures are shown. FE-SEM images of the TiO_2 powder sol gel and TNT films in various hydrothermal temperatures are shown. From Figure 3a, the diameter of the TiO_2 powder

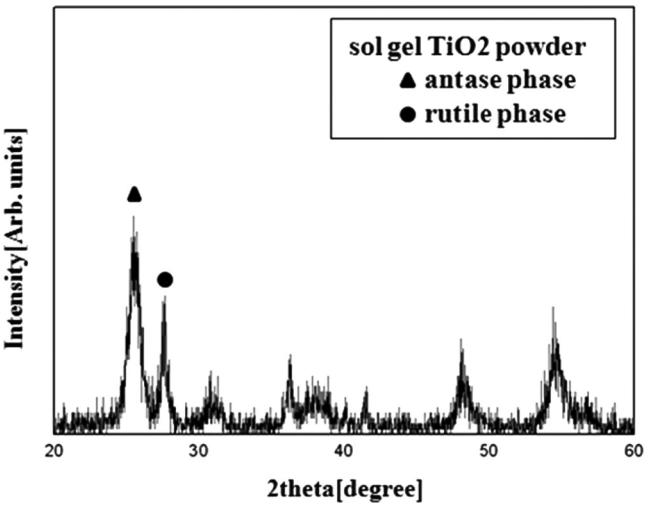

Figure 1. XRD patterns of the TiO_2 powder by sol-gel method. (▲: Anatase Phase, ●: Rutile Phase).

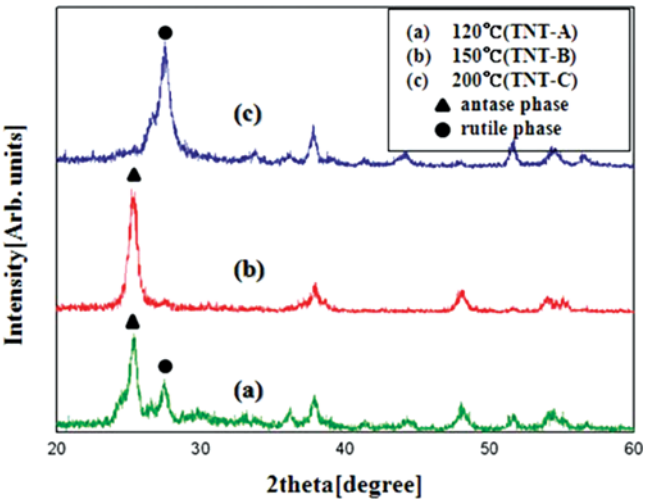

Figure 2. XRD patterns of the TiO_2 nanotube films at various hydrothermal temperatures. (a) 120°C, (b) 150°C, (c) 200°C (▲: Anatase Phase, ●: Rutile Phase).

prepared by the sol gel method is observed regularly to be 25 nm Figure 3b, c, and d. From the FE-SEM images, the TiO_2 particles exhibit tubular shapes. Figure 3b shows the FE-SEM image of TNT film prepared at 120°C. The diameter of TNT film at 120°C is observed to be 30 nm. Figure 3c shows the FE-SEM image of the annatase TNT film. Figure 3d reveals a 60 nm outer diameter for the rutile TNT film at 200°C. The SEM results show that the grain size of the rutile phase is larger than that of the anatase phase. It was observed that the TiO_2 film transformed into the rutile phase, as the hydrothermal temperature increases. This shows that it influences the size of the first particle.

Figure 4 shows the surface morphology of the TiO_2 film on FTO glass. The FE-SEM image shown clearly indicates that it is comprised of three parts. The top part is the TNT layer, followed by a 5 μm thick layer. No evidence of a second-phase interfacial layer between the TNT layer and the bottom FTO layer was found.

The absorption spectra of the photoelectrode affect dye adsorption on TNT film. Figure 5 shows the absorption spectra of dye N719 desorbed from the TiO_2 film electrodes contained with different hydrothermal temperatures. At 320 nm wavelength, the TNT prepared at TNT-B showed identical absorption of 3.644. The absorption of the TNT film at 120°C is slightly reduced in the region 300 nm∼800 nm compared to the TNT film prepared at 150°C. Increase in the TNT diameter leads to decrease in absorption. The absorption of the TNT film prepared at 200°C decreased to 2.497 at 320 nm wavelength.

The DSSCs were assembled using the photocurrent–voltage curves based on the optimal conditions of the TNTs film. Figure 6 shows the current density of the DSSCs measured under a simulated solar light irradiation of $100\,mW \cdot cm^{-2}$ (Table 1 and Fig. 6). A DSSC with light-to-electric energy conversion efficiency of 2.41%, short-circuit current density of $6.09\,mA \cdot cm^{-2}$, open-circuit voltage of 0.679 V and fill factor of 58.19% was achieved. For the TNT (150°C) film, the

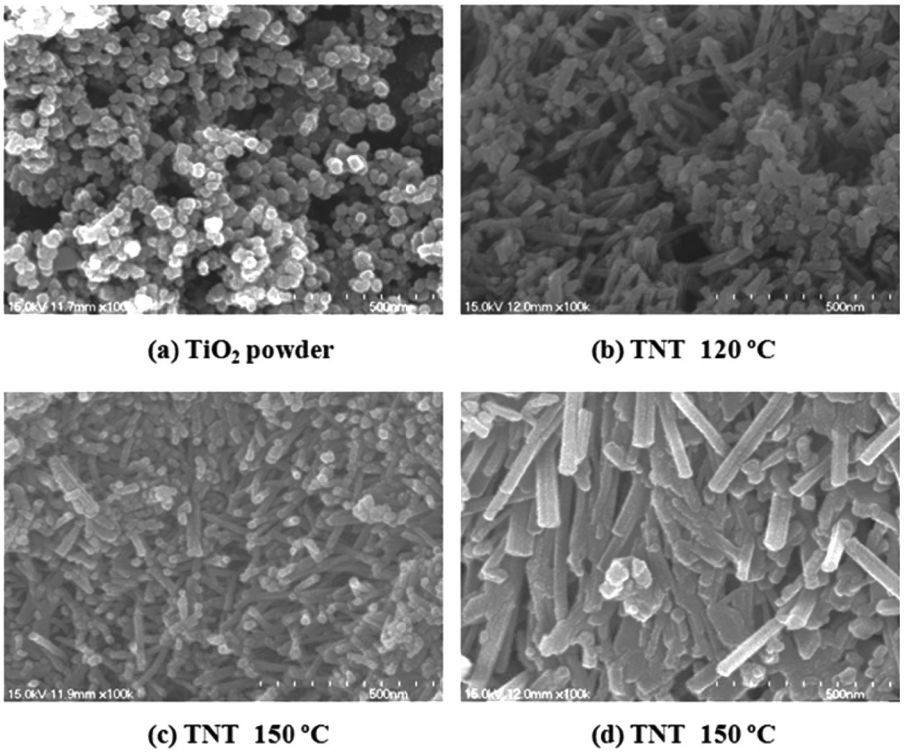

Figure 3. FE-SEM images of the TiO_2 power and TiO_2 nanotube films at various hydrothermal temperatures: (a) TiO_2 power, (b) 120°C, (c) 150°C, (d) 200°C.

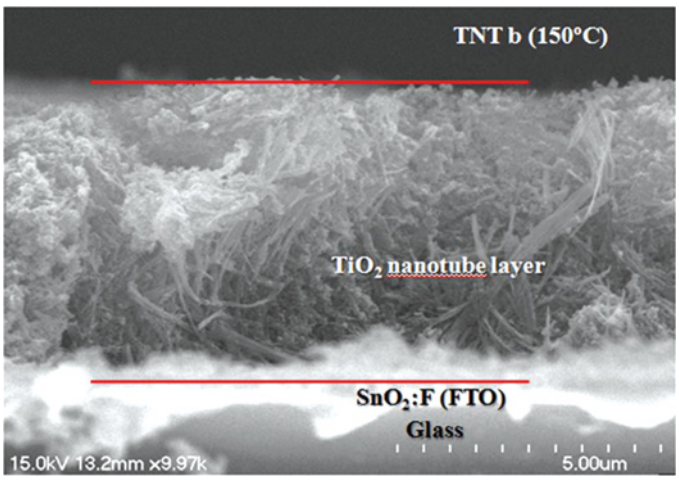

Figure 4. FE-SEM images showing a cross–sectional view of TiO_2 nanotube layer at 150°C.

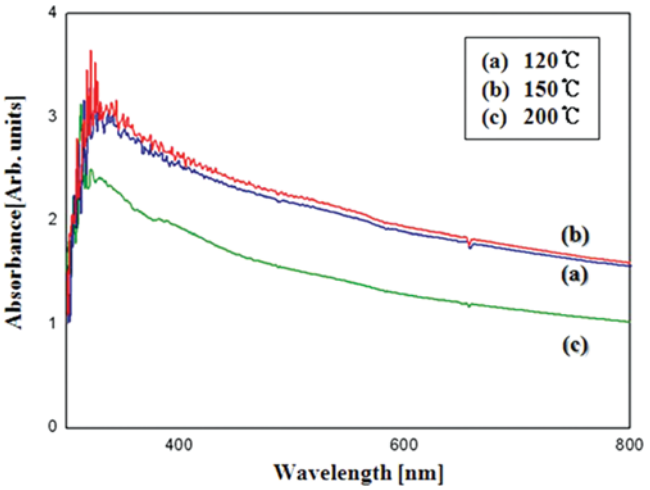

Figure 5. Absorption spectra of dye N719 desorbed from the TiO_2 film electrodes contained with different hydrothermal temperatures. : (a) 120°C, (b) 150°C, (c) 200°C.

conversion efficiency showed the best result. Higher absorbance means a higher dye concentration according to Lambert–Beer's law; a suitable amount of TNT in the film could provide a large surface area for the adsorption of the dye. It is well-known that the photocurrent of the flexible DSSC is correlated directly with the amount of the dye molecule; the more the dye molecules are adsorbed, the more incident light is harvested, and a larger photocurrent occurs. Our experiments demonstrate that TNT (150°C) adsorbs most dye N719 and produces a larger photocurrent.

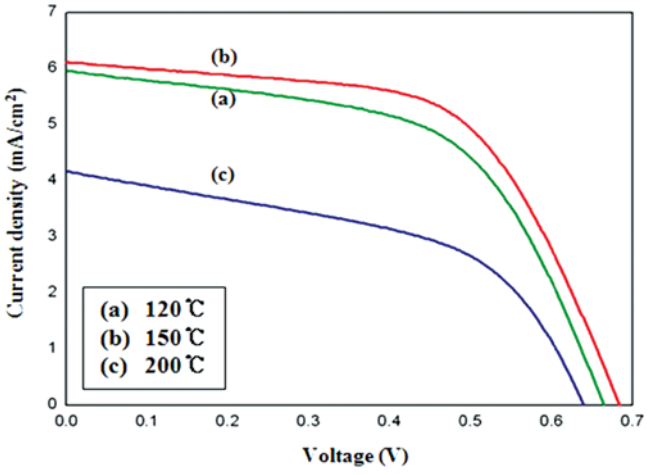

Figure 6. I-V characteristic of DSSC using TiO_2 nanotube films at various hydrothermal temperatures.

Table 1. Jsc, Voc, FF, and efficiency

Hydrothermal temperature (°C)	Jsc (mA/cm^2)	Voc (V)	Fill factor (%)	Efficiency (η)
120	5.89	0.622	56.77	2.25
150	6.09	0.679	58.19	2.41
200	4.18	0.648	52.72	1.43

Conclusion

TiO_2 nanotubes were successfully produced using a simple template-free sol-gel method and hydrothermal method. The properties of dye sensitized solar cells based on TiO_2 nanotube films deposited by screen printing have been studied. The anatase phase crystal property was found to be at its best at a hydrothermal temperature 120°C. The TiO_2 layers had more of the rutile phase with an increase of the hydrothermal temperature. The TiO_2 layer deposited was 5 μm thick. The variation of the photoelectric conversion efficiency in the solar cells with different TiO_2 layers is discussed, along with the analysis of the crystallite and optical properties of the films. The DSSC fabricated on an anatase phase TiO_2 layer deposited FTO electrode shows the highest conversion efficiency of 2.41%, since it prevents electron transfer to the electrolyte. From this it is deduced that as the hydrothermal temperature increases, the grain size and crystalline structure of the TiO_2 nanotube layer highly affect the DSSC conversion efficiency.

Acknowledgment

This work was supported by the Human Resources Development of the Korea Institute of Energy Technology Evaluation and Planning (KETEP) grant funded by the Korea government Ministry of Knowledge Economy (*No. 20104010100510*).

References

[1] Hamann, T. W., Jensen, R. A. A. B., Martinson, F., Ryswyk, H. V., & Hupp, J. T. (2008). *Energ. Environ. Sci.*, *1*, 66.
[2] Kong, F.-T., Dai, S.-Y., & Wang, K.-J. (2007). *Adv. Opto Elect.*, 75384.
[3] Durr, M., Schmid, A., Obermaier, M., Rosselli, S., Yasuda, A., & Nelles, G. (2005). *Naturematerials*, *4*, 607.
[4] Adachi, M., Murata, Y., Takao, J., Jiu, J., Sakamoto, M., & Wang, F. (2004). *J. Am. Chem. Soc.*, *126*, 14943.
[5] Kang, S. H., Kim, J. Y., Kim, Y., Kim, H. S., & Sung, Y. E. (2007). *J. Phys. Chem. C*, *111*, 9614.
[6] Solbrand, A., Lindstrom, H., Rensmo, H., Hagfeldt, A., Lindiquist, S.-E. (1997). *J. Phys. Chem.*, *101*, 2514–2518.
[7] Kambe, S., Nakade, S., Kitamura, T., Wada, Y., & Yanagida, S. (2002). *J. Phys. Chem. B*, *106*, 2967–2972.
[8] Dloczik, L., Ileperuma, O., Lauermann, I., Peter, L. M., Ponomarev, E., Redmond, G., Shaw, N. J., & Uhlendorf, I. (1997). *J. Phys. Chem. B*, *101*, 10281–10289.

[9] Fisher, A. C., Peter, L. M., Ponomarev, E. A., Walker, A. B., & Wijayantha, K. G. U. (2000). *J. Phys. Chem. B*, *104*, 949–958.
[10] Adachi, M., Murata, Y., Takao, J., Jiu, J., Sakamoto, M., & Wang, F. (2004). *J. Am. Chem. Soc.*, *126*, 14943–14950.
[11] Fisher, A. C., Peter, L. M., Ponomarev, E. A., Walker, A. B., & Wijayantha, K. G. U. (2000). *J. Phys. Chem. B*, *104*, 949–958.